Computational Mechanics 33 (2003) 61–67 © Springer-Verlag 2003
DOI 10.1007/s00466-003-0500-x

Finite element and asymptotic homogenization methods applied to smart composite materials

H. Berger, U. Gabbert, H. Köppe, R. Rodriguez-Ramos, J. Bravo-Castillero,

R. Guinovart-Diaz, J. A. Otero, G. A. Maugin

Abstract The piezoelectric effect is studied for bending and traction tests for two types of structure configurations: homogeneous and composite structures. Mechanical displacements are calculated for traction and bending tests, using FEM for the homogeneous body, where the input material properties are taken from the overall coefficients reported by the Asymptotic Homogenization Method (AHM). A brief theoretical description about the basics of the piezoelectric finite elements and the AHM is given. On the other hand, the calculations of the mechanical displacements are done for the composite structure using FEM where the real data of the material parameters for cylindrical fibers (PZT-5) embedded in a matrix (elastic isotropic polymer) were taken from reported references. A comparison between the results obtained using AHM + FEM and FEM for the homogeneous and the composite structures respectively is reported and shows a favorable result.

Keywords Finite element method, Asymptotic homogenization method, Piezoelectric composites, Heterogeneous structures

Received: 12 March 2003 / Accepted: 8 August 2003
Published online: 20 November 2003

H. Berger, U. Gabbert, H. Köppe
Otto-von-Guericke-Universitaet Magdeburg,
Fakultaet fuer Maschinenbau, Institut fuer Mechanik,
Universitaetsplatz 2, D-39106 Magdeburg, Germany

R. Rodriguez-Ramos, J. Bravo-Castillero[1], R. Guinovart-Diaz
Facultad de Matemática y Computación. Universidad de la Habana. San Lázaro y L, CP 10400, Vedado, Habana 4, Cuba

J. A. Otero
Instituto de Cibernética, Matemática y Física (ICIMAF)
Calle 15 e/t C y D, CP 10400, Vedado, Habana 4, Cuba

G. A. Maugin (✉)
Laboratoire de Modélisation en Mécanique,
Université Pierre et Marie Curie,
Case 162, 8 rue du Capitaine Scott, 75015 Paris, France
e-mail: gam@ccr.jussieu.fr

[1] *Present address*: Instituto Tecnológico de Estudios Superiores de Monterrey, Campus Estado de México, División de Arquitectura e Ingeniería, Apartado Postal 6–3, Atizapán de Zaragoza, 52926, Estado de México, México

The joint work has been started during a research stay of the author HB in Havana supported by the German Research Foundation (DFG). It was completed while the author RRR was visiting the Laboratoire de Modelisation en Mécanique at Université Pierre et Marie Curie, Paris. During this stay a visit to the Institute of Mechanics at Otto-von-Guericke-University of Magdeburg was supported by the Graduate Research Training Program "Micro-Macro Interactions in Structured Media and Particle Systems" from the German Research Foundation (DFG). G.A.M benefits from a Max-Plank Award for International Cooperation (2002–2005).

1 Introduction

Piezoelectric ceramics, such as lead zirconate–titanate (PZT), are widely used for transducers in sonar, underwater communications, underwater or medical imaging applications, as well as for control applications. Even if their properties make them interesting, they are often of limited use, first due to their weight, that can be a clear disadvantage for shape control, and, as a consequence, in reason of their high specific acoustic impedance, which reduces their acoustic matching with the external fluid domain.

For the last 20 years, composite piezoelectric materials have been developed by combining piezoceramics with passive nonpiezoelectric polymers [1–3]. Superior properties have been achieved by these composites by taking advantage of the most profitable properties of each of the constituents and a great variety of structures have been designed. Many models are available to describe these piezocomposites [4–6].

Recently, due to the design of piezocomposites on a greatly reduced scale and the use of PZT fibers instead of piezoelectric bars [7–10], new applications toward electromechanical sensors and actuators have become possible. But, because they are now much smaller than the wavelength of interest, homogenization techniques are necessary to describe the behavior of these piezocomposites [11–15].

On the other hand, numerical models seem to be well-suited to describe the behavior of these materials, because there is no restriction on the geometry, on the material properties, on the number of phases in the piezocomposite, and on the size. Therefore, the finite element method with the help of FEM system COSAR [16–22] has been used to solve problems concerning smart composite structures.

The aim of the present paper is the comparison between the FEM system and the theoretical approach reported by the asymptotic homogenization method (AHM) for two

different models. It is well known that AHM can provide overall material constants which describe the global behavior of the composite structure. In that case, we obtained certain equivalent homogeneous volume where the application of the FEM is more efficient instead of modeling a complicated heterogeneous structure. Therefore, in the present paper, using FEM, traction and bending tests for a homogeneous Ω and heterogeneous Ω' bodies are studied. Firstly, the traction and bending tests are calculated by FEM for the homogeneous structure Ω , using the effective coefficients derived by means of the asymptotic homogenization method (AHM) [14, 15] as input material parameters. Then, using FEM, traction and bending tests are computed for the same type of structure Ω but now reinforced with unidirectional piezoelectric cylindrical fibers embedded in a passive polymer, (denoted it Ω'). A comparison between the results derived by AHM+FEM (for homogeneous structure Ω) and FEM (for the heterogeneous structure Ω') is shown.

2
Piezoelectric finite element basics

More than often, the coupled electromechanical behavior of a piezoelectric smart material can be modeled with sufficient accuracy by means of linear constitutive equations. The linear constitutive equations for the piezoelectric materials can be written in the following form [23, 24]:

$$\begin{aligned} \sigma_{ij} &= \underbrace{C_{ijkl}u_{k,l}}_{\text{elasticity}} - \underbrace{e_{kij}E_k}_{\text{conv.piezoelectricity}} \\ D_i &= \underbrace{e_{ijk}u_{j,k}}_{\text{direct piezoelectricity}} + \underbrace{\kappa_{ij}E_j}_{\text{permittivity}} \end{aligned} \tag{2.1}$$

with C_{ijkl} – stiffness tensor, e_{kij} – piezoelectric tensor (relating stress to electric field), κ_{ij} – permittivity tensor, u_k – the components of the displacement vector, D_i – vector of the electric displacement, E_k is the electric field and σ_{ij} is the second order stress tensor. The basis for describing the coupled field behaviour is given by the balance law and Gauss' law respectively. In the absence of body forces and for quasi-electro-elastostatics these can be written as:

$$\sigma_{ji,j} = 0, \quad \sigma_{ij} = \sigma_{ji}, \quad D_{i,i} = 0 \ , \tag{2.2}$$

The boundary conditions on the surface S are required for giving a complete description of the coupled two-field problem. In this sense, the boundary conditions are supposed to be the union of partial surfaces, where no intersections are expected. Therefore, the boundary conditions can be written in the following form:

$$\begin{aligned} &u_i = \bar{u}_i - \text{displacement on } S_u, \\ &\sigma_{ji}n_j = \bar{t}_i - \text{traction on } S_\sigma \ , \end{aligned} \tag{2.3}$$

$$\begin{aligned} &\varphi = \bar{\varphi} - \text{surface potential on } S_\varphi, \\ &D_i n_i = -\bar{Q} - \text{surface charge on } S_D \ , \end{aligned} \tag{2.4}$$

where $(\bar{\cdot})$ are prescribed values, φ is the electric potential and Q is the electric charge.

The field Equations (2.2) as well as the boundary conditions (2.3) and (2.4), introducing the weighting quantities δu_i – virtual displacement, and $\delta\varphi$ – virtual electric potential, can be represented equivalently as follows:

$$\begin{aligned} \delta F_u = &- \int_V \delta u_{i,j}\left(C_{ijkl}u_{k,l} + e_{kij}\varphi_{,k}\right)\mathrm{d}V \\ &+ \int_{S_t} \delta u_i \bar{t}_i \, \mathrm{d}S = 0 \ , \end{aligned} \tag{2.5}$$

$$\begin{aligned} \delta F_\varphi = &- \int_V \delta\varphi_{,i}\left(e_{ijk}u_{j,k} + \kappa_{ij}\varphi_{,j}\right)\mathrm{d}V \\ &- \int_{S_Q} \delta\varphi\bar{Q} \, \mathrm{d}S = 0 \ . \end{aligned} \tag{2.6}$$

The field variables (u_e, φ_e) within a finite element (subscript e) can be approximated by means of the shape functions $(\mathbf{N}_u, \mathbf{N}_\varphi)$, described in local element coordinates ξ_i, and the unknown nodal degrees of freedom (u_k, φ_k) via the following relations:

$$\mathrm{u}_e = \mathrm{N}_u\left(\xi_1, \xi_2, \xi_3\right)\mathrm{u}_k, \quad \varphi_e = \mathrm{N}_\varphi\left(\xi_1, \xi_2, \xi_3\right)\varphi_k \tag{2.7}$$

For simplification purposes, the symbols

$$\mathrm{B}_u = \mathrm{D}_u\mathrm{N}_u, \quad \mathrm{B}_\varphi = \mathrm{D}_\varphi\mathrm{N}_\varphi \ , \tag{2.8}$$

are introduced, where D_u , D_φ are the differential matrices

$$\mathrm{D}_u = \begin{bmatrix} \partial/\partial x_1 & 0 & 0 \\ 0 & \partial/\partial x_2 & 0 \\ 0 & 0 & \partial/\partial x_3 \\ \partial/\partial x_2 & \partial/\partial x_1 & 0 \\ 0 & \partial/\partial x_3 & \partial/\partial x_2 \\ \partial/\partial x_3 & 0 & \partial/\partial x_1 \end{bmatrix}, \quad \mathrm{D}_\varphi = \begin{bmatrix} \partial/\partial x_1 \\ \partial/\partial x_2 \\ \partial/\partial x_3 \end{bmatrix} . \tag{2.9}$$

Assuming that $\delta F_u = \sum \delta F_u^e$, $\delta F_\varphi = \sum \delta F_\varphi^e$, the element energy functional results in

$$\begin{aligned} \delta F_u^e = &-\delta u_k^T \int_{V^e} \mathrm{B}_u^T C \mathrm{B}_u \, \mathrm{d}V u_k - \delta u_k^T \int_{V^e} \mathrm{B}_u^T e^T \mathrm{B}_\varphi \, \mathrm{d}V \varphi_k \\ &+ \delta u_k^T \int_{S_e^t} \mathrm{N}_u^T \bar{t} \, \mathrm{d}S = 0 \end{aligned} \tag{2.10}$$

$$\begin{aligned} \delta F_\varphi^e = &-\delta\varphi_k^T \int_{V^e} \mathrm{B}_\varphi^T e \, \mathrm{B}_u \, \mathrm{d}V u_k + \delta\varphi_k^T \int_{V^e} \mathrm{B}_\varphi^T \kappa \mathrm{B}_\varphi \, \mathrm{d}V \varphi_k \\ &- \delta\varphi_k^T \int_{S_Q^e} \mathrm{N}_\varphi^T \bar{Q} \, \mathrm{d}S = 0 \end{aligned} \tag{2.11}$$

With the abbreviations

$$\begin{aligned} K_{uu}^e &= \int_{V^e} \mathrm{B}_u^T C \mathrm{B}_u \, \mathrm{d}V, \quad \mathrm{K}_{u\varphi}^e = \int_{V^e} \mathrm{B}_u^T e^T \mathrm{B}_\varphi \, \mathrm{d}V, \\ \mathrm{K}_{\varphi u}^e &= \int_{V^e} \mathrm{B}_\varphi^T e \mathrm{B}_u \, \mathrm{d}V, \quad \mathrm{K}_{\varphi\varphi}^e = \int_{V^e} \mathrm{B}_\varphi^T \kappa \mathrm{B}_\varphi \, \mathrm{d}V \end{aligned} \tag{2.12}$$

$$f_u^e = \int_{O_t^e} \mathrm{N}_u^T \bar{t}\, \mathrm{d}O, \quad f_\varphi^e = -\int_{O_Q^e} \mathrm{N}_\varphi^T \bar{Q}\, \mathrm{d}O \tag{2.13}$$

for one finite element (superscript e) and assembling into a global matrix, the system equations can be written as

$$\begin{bmatrix} K_{uu} & K_{u\varphi} \\ K_{\varphi u} & -K_{\varphi\varphi} \end{bmatrix} \begin{bmatrix} u \\ \varphi \end{bmatrix} = \begin{bmatrix} f_u \\ f_\varphi \end{bmatrix} . \tag{2.14}$$

A library of powerful finite piezoelectric elements method for solving numerically coupled electromechanical problems has been included in the FEM system COSAR [21, 22]. The finite element library for piezoelectric controlled smart structures developed on the basis of the above given equations includes solid elements, plane elements, axisymmetric elements, rod elements [16, 17]. The shape functions of the finite elements can be linear or quadratic and the isoparametric element concept was used to approximate the element geometry. The solid element family consists of a basic brick-type element (hexahedron) and some special degenerated elements derived by collapsing nodes.

3
Asymptotic homogenization method (AHM)

The constitutive relations of the linear piezoelectricity theory for a heterogeneous and periodic medium Ω' are characterized by different material coefficients: C (elastic), e (piezoelectric) and κ (dielectric) which are X periodic functions. X denotes the periodic cell, whereas C, e and κ are of fourth, third and second order tensors. By means of the asymptotic homogenization method [11–15, 25] the original constitutive relations with rapidly oscillating material coefficients are transformed in two sets of mathematical problems. The first set has new physical relations over Ω with constant coefficients: $\bar{C}$ (elastic), $\bar{e}$ (piezoelectric) and $\bar{\kappa}$ (dielectric) which represent the properties of an equivalent homogeneous medium Ω and they are called the effective coefficients of the composite under study. They are calculated by using the following formulae [12]:

$$\bar{C}_{ijpq} = \left\langle C_{ijpq}(x) + C_{ijkl}(x)\,{}_{pq}M_{k,l}(x) + e_{kij}(x)\,{}_{pq}N_{,k}(x) \right\rangle,$$

$$\bar{e}_{ipq} = \left\langle e_{ipq}(x) + e_{ikl}(x)\,{}_{pq}M_{k,l}(x) - \kappa_{ik}(x)\,{}_{pq}N_{,k}(x) \right\rangle,$$

$$\overline{\kappa}_{ip} = \left\langle \kappa_{ip}(x) - e_{ikl}(x)\,{}_{p}Q_{,k}(x) + \kappa_{ik}(x)\,{}_{p}P_{k,l}(x) \right\rangle , \tag{3.1}$$

where $\langle f \rangle = \frac{1}{|X|}\int_X f \mathrm{d}Y$. The material coefficients $C_{ijpq}(x)$, $e_{ipq}(x)$, $\kappa_{im}(x)$ are known functions of the constituents composite phases. $x = (x_1, x_2, x_3)$ is the local variable on the periodic cell X . The subscripts assume the values 1, 2 and 3; the comma denotes partial differentiation, and the summation convention is applied. The second set allows the calculation of the functions, ${}_{pq}M$, ${}_{pq}N$, ${}_{p}P$ which are solutions of the so-called local problems ${}_{pq}L$ and ${}_{p}L$. The local problems ${}_{pq}L$ and ${}_{p}L$ are solved over the periodic cell X and they were derived in [11–15]. More precisely, this is dealt with as follows.

We consider a two-phase fiber-reinforced piezoelectric composite body, with the axis x_3 parallel to the cylindrical fibers (see Fig. 1b). The composite constituents are homogeneous linear transversely isotropic piezoelectric materials, with the axis of transverse isotropy oriented in the direction of the fibers. The cell X of the body is chosen with a side parallel to the x_3 direction and with unit length. The common interface between the fiber and the matrix is denoted by Γ.

The local problems ${}_{pq}L$ where the subscripts $p, q = 1, 2, 3$ and $pq = qp$, seeks the pq-displacement ${}_{pq}M^{(\alpha)}$ and the pq -potential ${}_{pq}N^{(\alpha)}$ in X_α, which are double periodic functions of periods $\omega_1 = (1, 0)$ and $\omega_2 = (0, 1)$ in the Ox_1, Ox_2 directions respectively. They are the solutions of

$$\begin{aligned}
&{}_{pq}\sigma^{(\alpha)}_{i\delta,\delta} = 0 \quad \text{in } X_\alpha;\\
&{}_{pq}D^{(\alpha)}_{\delta,\delta} = 0 \quad \text{in } X_\alpha;\\
&\left\|{}_{pq}M_i\right\| = 0 \quad \text{on } \Gamma; \ \left\|{}_{pq}N_i\right\| = 0 \quad \text{on } \Gamma;\\
&\left\|{}_{pq}\sigma_{i\delta}n_\delta\right\| = -\left\|C_{i\delta pq}\right\|n_\delta \quad \text{on } \Gamma;\\
&\left\|{}_{pq}D_\delta n_\delta\right\| = -\left\|e_{\delta pq}\right\|n_\delta \quad \text{on } \Gamma;\\
&\left\langle {}_{pq}M_i \right\rangle = 0, \quad \left\langle {}_{pq}N_i \right\rangle = 0 \ ,
\end{aligned}$$

where

$$\begin{aligned}
&{}_{pq}\sigma^{(\alpha)}_{i\delta} = C^{(\alpha)}_{i\delta k\lambda}\,{}_{pq}M^{(\alpha)}_{k,\lambda} + e^{(\alpha)}_{\lambda i\delta}\,{}_{pq}N^{(\alpha)}_{,\lambda};\\
&{}_{pq}D^{(\alpha)}_{\delta} = e^{(\alpha)}_{\delta k\lambda}\,{}_{pq}M^{(\alpha)}_{k,\lambda} - \kappa^{(\alpha)}_{\delta\lambda}\,{}_{pq}N^{(\alpha)}_{,\lambda};\\
&{}_{pq}\sigma^{(\alpha)}_{33} = C^{(\alpha)}_{3311}\,{}_{pq}M^{(\alpha)}_{\alpha,\alpha};\ {}_{pq}D^{(\alpha)}_{3} = e^{(\alpha)}_{311}\,{}_{pq}M^{(\alpha)}_{\alpha,\alpha},
\end{aligned}$$

and

$${}_{pq}\sigma^{(\alpha)}_{i\delta} = C^{(\alpha)}_{i\delta k\lambda}\,{}_{pq}U^{(\alpha)}_{k,\lambda} \ ;$$

the comma notation denotes a partial derivative relative to the x_δ component; the summation convention is understood, but it is taken only over repeated lower cases indices. X_a is the region occupied by the phase a. The outward unit normal vector to the interface Γ is $\mathbf{n}$. The double bar notation $\|f\|$ denotes the jump of the function f across the interface Γ, i.e. $\|f\| = f^{(1)} - f^{(2)}$ whereas the indices (1) and (2) denote the matrix and the fiber properties respectively.

The ${}_{p}L$ problems are stated as follows: the p-displacement ${}_{p}P^{(\alpha)}$ and the p-potential ${}_{p}Q^{(\alpha)}$ are sought in X_α, which are periodic functions of periods $\omega_1 = (1, 0)$ and $\omega_2 = (0, 1)$ that satisfy the boundary-value problems

$$\begin{aligned}
&{}_{p}\sigma^{(\alpha)}_{i\delta,\delta} = 0 \quad \text{in} \quad X_\alpha;\\
&{}_{p}D^{(\alpha)}_{\delta,\delta} = 0 \quad \text{in} \quad X_\alpha;\\
&\left\|{}_{pq}P_i\right\| = 0 \quad \text{on} \quad \Gamma; \ \left\|{}_{pq}Q_i\right\| = 0 \quad \text{on } \Gamma;\\
&\left\|{}_{p}\sigma_{i\delta}n_\delta\right\| = -\left\|e_{pi\delta}\right\|n_\delta \quad \text{on} \quad \Gamma;\\
&\left\|{}_{p}D_\delta n_\delta\right\| = -\left\|\kappa_{\delta p}\right\|n_\delta \quad \text{on} \quad \Gamma;\\
&\left\langle {}_{p}P_i \right\rangle = 0, \quad \left\langle {}_{p}Q_i \right\rangle = 0 \ ,
\end{aligned}$$

where

$$
\begin{aligned}
{}_p\sigma_{i\delta}^{(\alpha)} &= C_{i\delta k\lambda}^{(\alpha)}\, {}_pP_{k,\lambda}^{(\alpha)} + e_{\lambda i\delta}^{(\alpha)}\, {}_pQ_{,\lambda}^{(\alpha)};\\
{}_pD_{\delta}^{(\alpha)} &= e_{\delta k\lambda}^{(\alpha)}\, {}_pP_{k,\lambda}^{(\alpha)} - \kappa_{\delta\lambda}^{(\alpha)}\, {}_pQ_{,\lambda}^{(\alpha)};\\
{}_p\sigma_{33}^{(\alpha)} &= C_{3311}^{(\alpha)}\, {}_pP_{\alpha,\alpha}^{(\alpha)};\\
{}_pD_{3}^{(\alpha)} &= e_{311}^{(\alpha)}\, {}_pP_{\alpha,\alpha}^{(\alpha)} \ .
\end{aligned}
$$

The analytical solution of the local problems, which is based upon the complex-potential method of Muskhelishvili, utilizes a series expansion of the doubly periodic Weierstrass elliptic functions to predict both the local and overall averaging properties of the composite materials [26, 27].

Using the formula (3.1) we obtain for the plane-problem the following expressions for the global properties of the composite:

$$
\begin{aligned}
&\bar{k} = k_v - V_2\|k\|^2 K/m_1, \quad \bar{l} = l_v - V_2\|l\|\|k\|K/m_1 \ ,\\
&\bar{n} = n_v - V_2\|l\|^2 K/m_1, \quad \bar{m} = m_v - V_2\|m\|M \ ,\\
&\bar{q} = q_v - V_2\|q\|\|k\|K/m_1, \quad \bar{r} = r_v - V_2\|l\|\|q\|K/m_1,\\
&\bar{u} = u_v + V_2\|q\|^2 K/m_1 \ .
\end{aligned}
\tag{3.2}
$$

In those formulae the coefficients $k = (C_{1111} + C_{1122})/2$, $l = C_{1133} = C_{2233}, m = (C_{1111} - C_{1122})/2$ and $n = C_{3333}$ corresponds to elasticity. The coefficients $q = e_{311} = e_{322}$ and $r = e_{333}$ are piezoelectric ones, and $u = \kappa_{33}$ is a dielectric constant. The subscripts v refers to the Voigt average of the relevant quantity, i.e., the phase-mixing rule in the cross section of the composite. For instance, $k_v = k_1V_1 + k_2V_2$, etc., and V_α are the area fractions occupied by the matrix and fiber materials, respectively, and $V_1 + V_2 = 1$. The constants K and M are calculated according to the expressions (3.36) and (3.38b) (see pp. 231–232, [13]) and the rest of effective properties $p = C_{1313}$, $s = e_{113}$ and $t = \kappa_{11}$ related to the anti-plane problem ${}_13L$ are computed following the formulae (3.26) (see pp. 244, [14]).

4
Numerical examples

In this section the piezoelectric effect is studied for bending and traction tests under different structure configurations. Homogeneous Ω and heterogeneous Ω' structures are analyzed. The homogeneous body Ω (Fig. 1) and its reinforcement by unidirectional piezoelectric cylindrical fibers which are periodically distributed in a polymer matrix, denoted by Ω' (Fig. 1), are studied. The diameter of the fibers, for the calculations, was stepwise changed which is directly related to the values of the volume fraction of the fibers. A column cross section illustrates the ratio volume fraction of the fibers and matrix respectively (see Fig. 2).

Two types of numerical simulations are presented. Firstly, the mechanical displacements were calculated for traction and bending tests, using FEM for the homogeneous body Ω (Fig. 1) where the input material properties are taken from the homogenized coefficients reported in (3.2). For simplicity, this case is so called AHM+FEM. Afterwards, the calculations of the mechanical displacements were done for the heterogeneous structure Ω' (Fig. 1) using FEM where the real data of the material parameters for cylindrical fibers (PZT-5) and matrix (elastic isotropic polymer) were taken from [28, 29]. This other case is called FEM. A comparison between the results obtained using AHM+FEM and FEM for the homogeneous and heterogeneous structures respectively is reported.

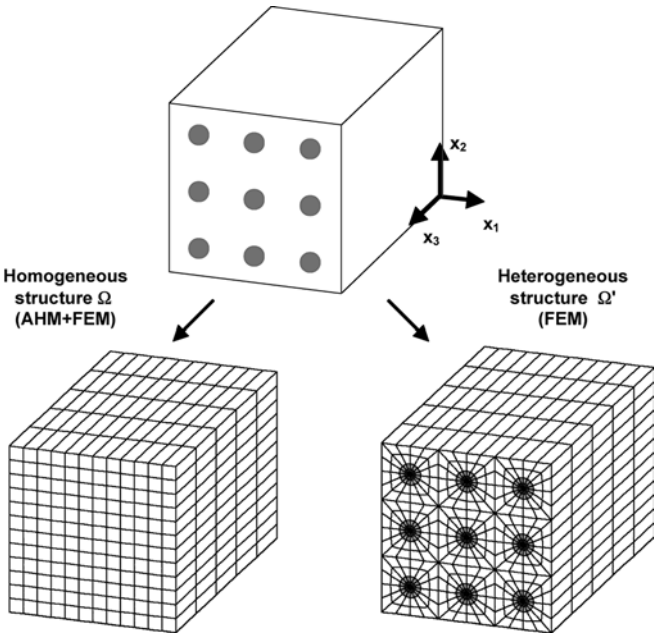

Fig. 1. Models of homogeneous Ω and heterogeneous Ω' structures

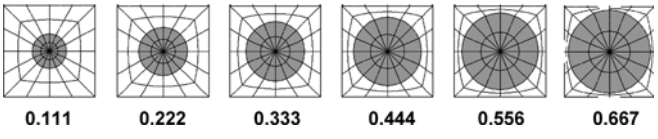

Fig. 2. Column cross section to show the ratio volume fraction between fibers and matrix in the composite used in the calculations

The input material parameters used in AHM+FEM and FEM are shown in Tables 1 and 2 respectively. It can obviously be seen that the effective coefficients in Table 2 calculated by AHM lie between the two extrema of the pure components listed in Table 1.

The mechanical displacements under traction and bending tests are calculated for six values of the volume fraction of the fibers (Fig. 2) using a block of 9 square cells in the composite Ω'. One cell has a size of $1 \times 1 \times 5$ mm.

In order to study the mechanical response to the electric source, both structures are clamped on one side as can be seen in Figs. 3 and 4. Traction and bending effects are induced by a difference of electric potential between the two end faces of the structures (see also Fig. 3 and 4). For the bending case the homogeneous structure is vertically divided in three isolated layers represented by a double

Table 1. Input parameters used in AHM+FEM. The parameters have been taken from [26, 27]. The dimensions of the parameters are: elastic constants [10^{10} N/m^2], piezoelectric constants [C/m^2] and dielectric constants [10^{-8} F/m]

	C_{11}	C_{12}	C_{13}	C_{33}	C_{44}	e_{15}	e_{13}	e_{33}	κ_{11}	κ_{33}
PZT-5	12.1	7.54	7.52	11.1	2.11	12.3	−5.4	15.8	0.811	0.735
Polymer	0.386	0.257	0.257	0.386	0.064	–	–	–	–	–

Table 2. Input parameters used in FEM. The overall material properties (denoted by bar on the coefficients) were calculated by (3.2) using the asymptotic homogenization method. The dimensions of the parameters are: elastic constants [10^{10} N/m^2], piezoelectric constants [C/m^2] and dielectric constants [10^{-8} F/m]

Volume fraction	$\bar{C}_{11}$	$\bar{C}_{12}$	$\bar{C}_{13}$	$\bar{C}_{33}$	$\bar{C}_{44}$	$\bar{C}_{66}$	$\bar{e}_{15}$	$\bar{e}_{33}$	$\bar{e}_{13}$	$\bar{\kappa}_{11}$	$\bar{\kappa}_{33}$
0.111	0.445229	0.290051	0.292281	0.986351	0.079429	0.077589	0.001065	2.194286	−0.026231	0.009933	0.091959
0.222	0.520706	0.331912	0.337142	1.594029	0.099097	0.094396	0.002767	4.383125	−0.059585	0.012456	0.175912
0.333	0.620971	0.385865	0.396103	2.212487	0.125116	0.117553	0.005628	6.563949	−0.103422	0.015822	0.259805
0.444	0.761822	0.456846	0.477091	2.847789	0.161506	0.152487	0.010859	8.732250	−0.163637	0.020584	0.343606
0.556	0.974292	0.554232	0.595557	3.511748	0.217285	0.210030	0.021904	10.879245	−0.251715	0.028018	0.427248
0.667	1.327801	0.701985	0.787201	4.231662	0.318867	0.312908	0.052676	12.984637	−0.394201	0.042031	0.510580

line in the right part of Fig. 5, where the difference of the electric potential is applied as shown in Fig. 3b, creating thus a transverse electric field.

The traction in the composite is excited by a difference of electric potential applied on the fibers, 0 volt at the clamped side and –1 V at the opposite side of Ω', see Fig. 4a. On the other hand, the bending is induced by a difference of electric potential applied on the fibers of the free side of Ω' as well. Different values of the electric potential are applied, i.e. –1 V in the upper part, 0 V in the center and +1 V to the lower part of the composite. The fibers of the clamped side of the composite received an electrical load of 0 V as shown Fig. 4b. The applied electrical boundary conditions cause in the first case an elongation of the structure in x_3 direction (traction) and in the second case a deflection of the free end in negative x_2 direction (bending). The bending effect is induced by stretching of the upper layer and shortening of the lower layer.

The mechanical boundary conditions used in the calculations by FEM for traction and bending tests can be summarized as follows: clamping on one side ($u_3 = 0$ and in the direction 1 and 2 only the rigid body motion is avoided, free contraction is possible) and free on the other side (stress equals to zero) of the structures. Electric boundary conditions were prescribed previously (see Figs. 3 and 4).

Figure 5 shows the reference points of the mechanical displacements for traction and bending tests marked in the deformed heterogeneous structures Ω'. These reference points are used to compare the numerical results between homogeneous and heterogeneous models. Three points of reference for the bending test and one point of reference for the traction test are considered.

Figure 6a displays the comparison of the mechanical displacements component u_3 for the traction test calculated by AHM+FEM for the homogeneous structure Ω and the results reported by FEM in the composite Ω'. The relative error for the displacements between both methods

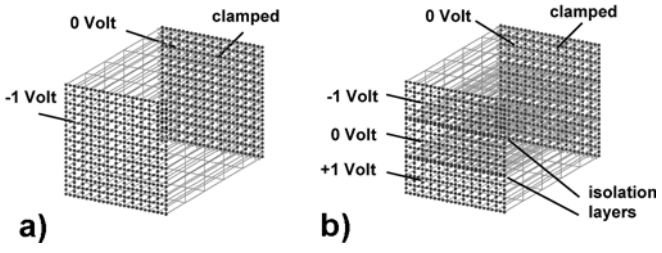

Fig. 3. Electric potential applied to the homogeneous structure for each test. **a** Traction test, **b** bending test

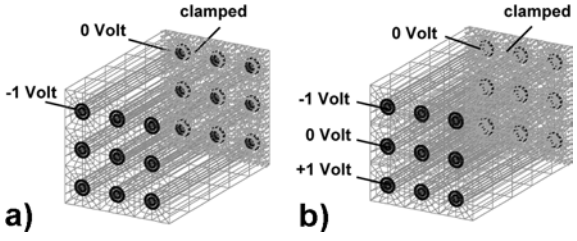

Fig. 4. Electric potential applied to the heterogeneous structure for each test. **a** Traction test, **b** bending test

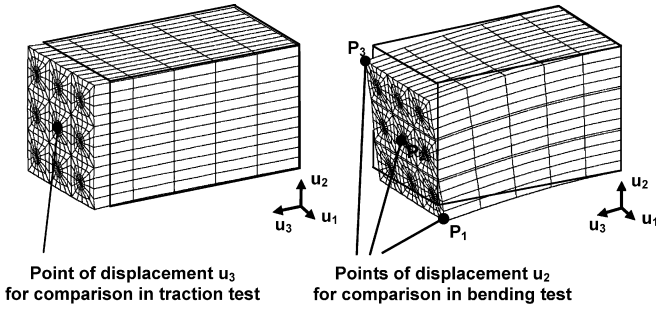

Fig. 5. Reference points of the mechanical displacements for traction and bending tests marked in the deformed heterogeneous structure Ω'. Three points for bending test and one point for traction test are considered

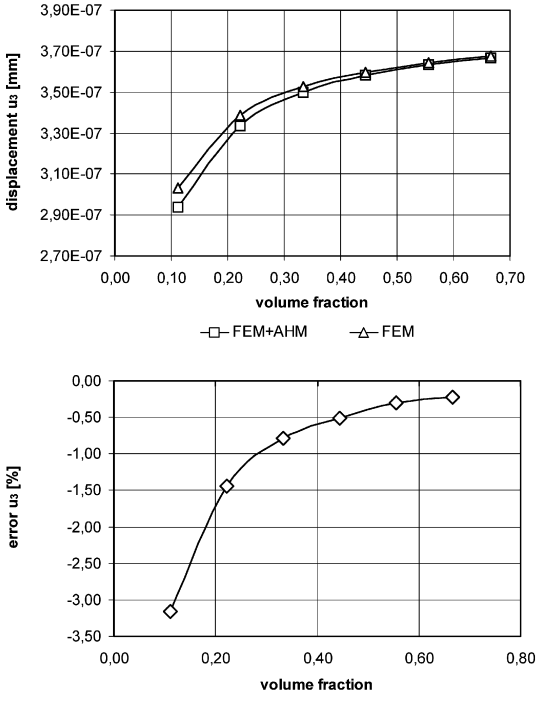

Fig. 6. **a** Comparison of the mechanical displacement u_3 for traction test calculated by AHM+FEM on Ω and the results reported by FEM on Ω'. **b** The relative error for the mechanical displacement u_3 between both methods is shown

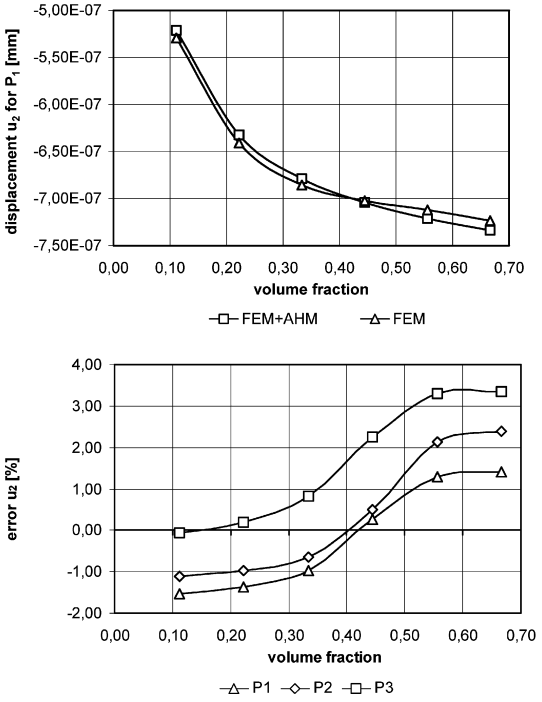

Fig. 7. **a** Comparison of the mechanical displacement u_2 for bending test calculated by AHM+FEM on Ω and the results reported by FEM on Ω'. **b** The relative error for the mechanical displacement u_2 between both methods is shown

is shown in Fig. 6b. This relative error is expressed in percentage where the formula is

$$\text{error}(u_3) = \left(\frac{u_3(\Omega) - u_3(\Omega')}{u_3(\Omega')} \times 100\% \right) \ .$$

Analogously, Fig. 7a exhibits the comparison of the mechanical displacements component u_2 for the bending test calculated by AHM+FEM for the homogeneous structure Ω and the calculations obtained by FEM in the composite Ω' in reference point P1. The relative error for the displacement u_2 between both methods is shown in Fig. 7b. In order to give the idea of the accuracy of the results, the relative error of the displacement u_2 is calculated for three different points located in three positions as shown in Fig. 5. The relative error of the displacement is defined as follows:

$$\text{error}(u_2) = \left(\frac{u_2(\Omega) - u_2(\Omega')}{u_2(\Omega')} \times 100\% \right) \ .$$

As can be seen from both tests, there exist a good agreement between the calculation of the displacements by using a homogeneous model with homogenized material coefficients calculated by AHM and a heterogeneous model using the real material constants for fibers and matrix. The relative error of the displacements reported in both tests is significantly small. In this sense it is possible to analyze more complex fiber reinforced piezoelectric structures with sufficient accuracy by using homogenized models. This allows one to create finite element models without detailed geometrical modeling of the fibers which reduces the effort for model generation and also for calculation in a drastic manner. Furthermore it is possible to vary the volume fraction of fibers in a simple way because only the material constants have to be changed in the finite element model.

5 Conclusions

A comparison between FEM using COSAR version and AHM have been reported. The piezoelectric effect has been analyzed for two types of problems, i.e., traction and bending tests for a piezoelectric homogeneous structure and a piezoelectric composite. The electromechanical response is calculated using AHM+FEM for the homogeneous structure and FEM for the composite. There exists good agreement between the two methods applied to both piezoelectric structures under traction and bending tests. The relative error of the displacements reported in both tests is significantly small. The numerical calculations have shown that using homogenized material constants calculated by AHM for modeling of composite structures by FEM is a very suitable technique.

References

1. **Newnham RE, Skinner DP, Cross LE** (1978) Connectivity and piezoelectric–pyroelectric composites. Mater. Res. Bull. 13: 525–536
2. **Gururaja TR, Schulze WA, Cross LE, Newnham RE, Auld BA, Wang YJ** (1985) Piezoelectric composite materials for ultrasonic transducer applications. Part I: resonant modes of vibration of PZT rod-polymer composites. IEEE Trans. Sonics Ultrason. SU-32: 481–498
3. **Gururaja TR, Schulze WA, Cross LE, Newnham RE** (1985) Piezoelectric composite materials for ultrasonic transducer applications. Part II: evaluation of ultrasonic medical applications. IEEE Trans. Sonics Ultrason. SU-32: 499–513

4. **Smith WA, Shaulov AA, Singer BM** (1984) Properties of composite piezoelectric materials for ultrasonic transducers. Proc. IEEE Ultrason. Symp. (IEEE, New York), pp. 539–544
5. **Hayward G, Hossack JA** (1990) Unidimensional modeling of 1–3 composite transducers. J. Acoust. Soc. Am. 88: 599–608
6. **Smith WA** (1993) Modeling 1–3 composite piezoelectrics: hydrostatic response. IEEE Trans. Ultrason., Ferroelec., Freq. Contr. 40(1): 41–49
7. **Bent AA, Hagood NW** (1997) Piezoelectric fiber composites with interdigitated electrodes. J. Intell. Mater. Syst. Struct. 8: 903–919
8. **Steinhausen R, Hauke T, Beige H, Watzka W, Lange U, Sporn D, Gebhardt S, Schönecker A** (2001) Properties of fine scale piezoelectric PZT fibers with different Zr content. J. Eur. Ceram. Soc. 21: 1459–1462
9. **Smith WA, Auld BA** (1991) Modeling 1–3 composite piezoelectrics: thickness-mode oscillations. IEEE Trans. Ultrason., Ferroelec., Freq. Contr. 38(1): 40–47
10. **Helen Lai Wah Chan, Unsworth J** (1989) Simple model for piezoelectric ceramic/polymer 1–3 composites used in ultrasonic transducer applications. IEEE Trans. Ultrason., Ferroelec., Freq. Contr. 36(4): 434–441
11. **Guinovart-Diaz R, Bravo-Castillero J, Rodriguez-Ramos R, Sabina FJ** (2001) Closed-form expressions for the effective coefficients of a fiber-reinforced composite with transversely isotropic constituents – I. Elastic and hexagonal symmetry. J. Mech. Phys. Solids 49: 1445–1462
12. **Sabina FJ, Rodriguez-Ramos R, Bravo-Castillero J, Guinovart-Diaz R** (2001) Closed-form expressions for the effective coefficients of a fiber-reinforced composite with transversely isotropic constituents – I. Piezoelectric and hexagonal symmetry. J. Mech. Phys. Solids 49: 1463–1479
13. **Rodriguez-Ramos R, Guinovart-Diaz R, Sabina FJ, Bravo-Castillero J** (2001) Closed-form expressions for the effective coefficients of fiber-reinforced composite with transversely isotropic constituents – I. Elastic and square symmetry. Mech. Mat. 33: 223–235
14. **Bravo-Castillero J, Sabina FJ, Guinovart-Diaz R, Rodriguez-Ramos R** (2001) Closed-form expressions for the effective coefficients of fiber-reinforced composite with transversely isotropic constituents – II. Piezoelectric and square symmetry. Mech. Mat. 33: 237–248
15. **Guinovart-Diaz R, Bravo-Castillero J, Rodriguez-Ramos R, Sabina FJ, Martinez-Rosado R** (2001) Overall properties of piezocomposite materials 1–3. Mat. Lett. 48: 93–98
16. **Berger H, Cao X, Köppe H, Gabbert U** (1998) Finite element based modelling and analysis of structronic systems. Proc. Conf. Smart Structures Witpress, Rome, pp. 67–76
17. **Berger H, Gabbert U, Köppe H** (2000) Designing precision smart structures by the finite element method. In: Proceedings of the 10th Int. Conference on Adaptive Structures and Technologies (ICAST'99, Paris, France), Bernadou M, Ohayon R (eds), Technomic Publishing Comp., Lancaster, USA, pp. 501–507
18. **Berger H, Gabbert U, Köppe H, Seeger F** (2000) Finite element analysis and design of piezoelectric controlled smart structures. J. Theor. Appl. Mech. 3(38): 475–498
19. **Berger H, Köppe H, Gabbert U, Seeger F** (2001) On finite element analysis of piezoelectric controlled smart structures. In: Smart Structures and Structronic Systems, Gabbert U, Tzou H-S (eds), Kluwer Academic Publisher, pp. 189–196
20. **Gabbert U, Köppe H, Seeger F, Berger H** (2002) Modeling of smart composite shell structures. J. Theor. Appl. Mech. 3(40): 575–593
21. **Berger H, Cao X, Köppe H, Gabbert U** (1998) Finite element based analysis of adaptive structures. In: Modelling and Control of Adaptive Mechanical Structures, Gabbert U (ed.). VDI-Fortschritt-Berichte, Reihe 11. Schwingungstechnik 268: 95–104
22. **Köppe H, Gabbert U, Tzou HS** (1998) On three-dimensional layered shell elements for the simulation of adaptive structures. In: Modelling and Control of Adaptive Mechanical Structures, Gabbert U (ed.), VDI-Fortschritt-Berichte, Reihe 11: Schwingungstechnik 268: 125–136
23. **Mindlin RD** (1961) On the equations of motion of piezoelectric crystals. In: Problems of Continuum Mechanics, Radock JRM (ed.), Philadelphia: SIAM 282–290
24. **Maugin GA** (1988) Continuum Mechanics of Electromagnetic Solids. North-Holland, Amsterdam
25. **Bensoussan A, Lions JL, Papanicolaou G** (1978) Asymptotic Analysis for Periodic Structures. North-Holland, Amsterdam
26. **Meguid SA, Kalamkarov AL** (1994) Asymptotic homogenization of elastic composite materials with a regular structure. Int. J. Solids Struct. 31: 303–316
27. **Pobedria BE** (1984) Mechanics of Composite Materials. Moscow State University Press, Moscow (in Russian)
28. **Dunn ML, Taya M** (1993) Micromechanics predictions of the effective electroelastic moduli of piezoelectric composites. Int. J. Solids Struct. 30: 161–175
29. **Dunn ML, Taya M** (1993) An analysis of piezoelectric composite materials containing ellipsoidal inhomogeneities. Proc. R. Soc. London. A 443: 265–287